MELLÉKLET

ATOMKI KÖZLEMÉNYEK

21. kötet 2. szám

MTA
ATOMMAG KUTATÓ INTÉZETE
DEBRECEN

1979

539 HU ISSN 0004-7155

MELLÉKLET

ATOMKI

KÖZLEMÉNYEK

21. kötet 2. szám

ATOMKI Közlemények Suppl. 21/2 (1979)1-53

DEVELOPMENT OF ETCHED NUCLEAR TRACKS*

G. SOMOGYI

Institute of Nuclear Research
of the Hungarian Academy of Sciences
Debrecen, Hungary

Abstract. The theoretical description of the evolution of etched tracks in solid state nuclear track detectors is considered for different initial conditions, for the cases of constant and varying track etch rates, isotropic and unisotropic bulk etching as well as for thick and thin detectors. It is summarized how one can calculate the main parameters of etch-pit geometry, the track length, the axes of a surface track opening, track profile and track contour. The application of the theory of etch-track evolution is demonstrated with selected practical problems. Attention is paid to certain questions related to the determination of unknown track parameters and calculation of surface track sizes. Finally, the theory is extended to the description of the perforation and etch-hole evolution process in thin detectors, which is of particular interest for track radiography and nuclear filter production.

*This paper was presented as an invited survey lecture at the International Spring School on the Development and Applications of Solid State Nuclear Track Detectors held at Islamabad (Pakistan), March 5-14, 1979.

CONTENT

1. INTRODUCTION

Numerous applications of solid state nuclear track detectors to the present and future needs of users and "trackologists" have become apparent. Consequently, more and more researchers raise a claim to get more experimental and also theoretical information about the behaviour of etched nuclear tracks. In view of this consideration I am very greatly honoured to be invited here to try to satisfy, even if only partially, one half of this demand.

One of the aim of my lecture is to provide a survey about our present possibilities for the theoretical description of the main problems related to the evolution of etched nuclear tracks. In other words I will examine here the etch-pit geometry and try to show how this geometry affects quantitatively several measurable track parameters like track length, axes of surface track opening, shape of the profile and contour of etch-pit. Attention will be mostly focused on the basic principles and relations governing etch-track evolution under different initial conditions (isotropic and unisotropic bulk etching, constant and varying track etch rate, thick and thin detectors). With knowledge of the principles and quantitative relations concerning the kinetics of track etching, I also intend to familiarize the participants of this Spring School with several, specific questions of track-evolution which may appear the most likely to be

usefully utilized in their future work. Of particular interest in this respect are the problems of the calculation of different track quantities in terms of measurable etch-pit parameters for nuclear particle identification, track radiography and nuclear filters.

It is to be emphasized that my survey is necessarily incomplete, and it should be considered only as a review of some of the most important ideas and assumptions on the subject which have been mostly reported on by other researchers and myself. In respect of detailed information I refer to the basic literature available on the geometry of etched nuclear tracks [1, 2, 3, 4, 5, 6]. For those who whish to understand, more deeply, the details of the calculation of some relations, my survey gives only a logical basis on the strength of which the participants of this Spring School may solve the problems as an "amusing homework". My lecture, to some extent, is also devoted to a certain systematization of the kinetics of etch-track growth, so full proofs of formulas will be given only in exceptional cases when they can be considered to be of "higher educational value".

2. BASIC CONSIDERATIONS

Let me begin by summarizing briefly and schematically the way which leads to the kinetics of etch-track growth. In Fig.1 a simple scheme is illustrated showing the "milestones" along this way. At the two ends we have the particle parameters (charge, mass, energy) as input data and

the etch-track parameters (length, axes, profile, contour) as the output ones. Along the way we can meet the response of the detector on microscopic and macroscopic levels in the course of the radiation damage and the chemical etching process, respectively. In order to understand clearly how this scheme works in practice, we have to find out the fundamental relations existing between the main parameters of the directly connected milestones.

At present there is a variety of proposed $S = f(P)$ functions that relate radiation damage quantities to the nuclear particle parameters. In the practice of different laboratories the use of the primary ionization and the restricted energy loss is equally preferred and justified [7]. However still more effort is required to find the conceptually correct damage quantity which is responsible for the preferential etchability.

There is a large gap in our present knowledge of the next fundamental relation, $V(S)$, which is frequently referred to in the literature as response function, and which gives the connection between the etching and the damage response of a detector. Our present knowledge of this function is almost completely empirical and little effort has been still made to describe theoretically the expectable variation of the etch-rate ratio along the damage trails and specially in terms of detector and etching parameters.

The finding of a proper response function is a central problem in any quantitative work with a given track de-

tector. For an adequate expression acceptable in practical work the criterion of self-consistency

$$V(S,Z_1) = V(S,Z_2) = ... = V(S,Z_i) \qquad (1)$$

should be satisfied as much as possible, i.e. with the same damage etching response should be independent of nuclear charge. Having a reasonable etch-rate ratio vs damage curve and using a range-energy relation, R(E), one can derive a set of etch-rate ratio vs residual range curves, V(R), for different nuclear particles, the knowledge of which is of primary importance in any kind of calculation related to the geometry of etched tracks.

The basic relation for the understanding of the development of the geometry of etched nuclear tracks can be represented by the function $T = f(V,h,\Theta,R_o)$ indicated in Fig.1. The determination of such functions for different experimental conditions can be considered as a basic task of the theory of etched track evolution during the chemical etching process (i.e. etch-track kinetics). It is my present task to demonstrate the capabilities of such a theory for typical cases. First of all, however, for the sake of an easier explanation of the topic, it is advisable to introduce a reasonable systematization for the variety of etch-track kinetics. Our systematization applied in this review is shown in Fig.2.

At first distinction should be made between etch-pit formation in track detectors with isotropic and unisotropic bulk etching rate (henceforth isotropic and un -

isotropic solids). The criterion of isotropic bulk etching is completely satisfied for glasses and in most of the cases with good approximation for high polymers if they are not oriented along a preferred direction during foil production. The unisotropic case is obviously represented by crystals, where the bulk etch rate is a complex function of the crystal plane orientation.

The second distinction is made according to the degree of alteration of the track etch rate along the nuclear track. This may be considered a computation technical simplification, because V_T actually varies along the trajectory of particles in most track detectors. In certain practical cases, however, it is a justifiable assumption to approximate V_T with a constant value, for which condition all relations of etch-track kinetics can be expressed in explicit, well-computable closed formulas.

The situations when V_T may be approximated as a constant are generally restricted to small layer removals and to track portions of higher energy particles where the damage density is only a slowly varying function of the range. In certain cases, however, when the calcu - lation of a given track parameter is not very sensitive to the changes in the value of V_T, one may usefully apply the etch-track kinetics with constant etch-rate ratio, even if V_T displays a sharply changing character. Such a situation arises for example in track axis calculations if the $V(x) > 10$ condition is satisfied.

In the end, from the point of view of etch-track kinetics, one can distinguish the cases which are related to thick and thin detectors where, by definition, the thin detector represents the case when during etching the foil is perforated through completely. It should be noted that for etch-track kinetics in thin foil there is no literary data available. Recently, however, it has become clear that it is most desirable to extend the theoretical description to the problem of film perforation and the hole evolution process, too. Having this in sight, at the end of my review, I intend to give a preliminary account of the results achieved in this field in our laboratory.

3. STARTING PARAMETERS

Before working out methods for giving the basic equations $T = f(V,h,\theta,R_o)$ of etch-track kinetics, a few words should be devoted to several important starting parameters of the theory, namely to the etch-rate ratio, critical angle and critical layer removal.

Etch-rate ratio. A satisfactorily quantitative and practically computable treatment of our problem can be obviously accomplished only with the knowledge of the complete form of the relation $V(R)$. A specially important question which arises here is how we can take into account the so-called "threshold region", i.e. the hardly etchable track portions.

As a part of a comprehensive study [8] we have shown that sound reasons force us to suppose that no sharp regis-

tration threshold exists, although the threshold concept has been a useful general classification guide for nuclear track detectors according to sensitivity. The existence of a registration threshold cannot be accepted, at least almost certainly, for pure pólymeric materials or foils containing relatively small amounts of additives. In a recent work further evidence is given that there is no sharp threshold for track production, and even tracks of 0,02 MeV protons can be observed in LR-115 cellulose nitrate providing the use of a sufficiently long etching time [9]. In a detailed study Price et al [10] have shown that even for mineral detectors there is no evidence for a "critical ionization rate" and the etching response is a smooth function of the radiation damage density along the track.

In the end, one can conclude that for the description of etch-track kinetics one should choose V(R) functions approaching the V=1 value (threshold criterion) gradually at increasing residual ranges. In Fig.3 such V(R) curves deduced from our studies for alpha-particle tracks are presented, clearly showing the absence of a well-definable threshold in the plastics studied. A reasonable representation of these curves can be given by the relation of the form

$$V = 1 + \exp(-AR+B) \qquad (2)$$

for PC, CA and CN and by the formula

$$V = 1 + A\,R^{-B} \qquad (3)$$

for CR-39 homopolymer, which has been recently found to be an exceptionally sensitive detector material [11]. where A and B are fitting parameters. It must be noted that eq. (2) seems also to be applicable for CR-39 but only in a portion of the alpha-particle residual range between about 8-40 μm. Generally, if no other simpler function is found, the use of the expression

$$V^{-1} = 1 - \sum_i A_i \exp(-B_i R) \qquad (4)$$

may be proposed for both light and heavy ions. With this and also with eq. (2) one can easily calculate the integral of type

$$H(x) = \int V^{-1}(x)\,dx \qquad (5)$$

which frequently appears in the relations of etch-track kinetics at varying etch-rate ratio along the range of particle.

Critical angle and critical layer removal. Considering a constant etch-rate ratio, the evolution of track geometry can be relatively easily followed at any incident angle as a result of the competition between the track and bulk etching effects. Only a critical angle given by

$$\Theta = \arcsin V_B/V_T \qquad (6)$$

should be taken into account as a limit angle for revealing tracks. At varying etch-rate ratios, however, the situation is obviously more complicated. Here, instead of the critical angle, it is more advisable to introduce a so-called critical layer removal, h_c, into the theoretical formalism. A demonstrative presentation of the meaning of

this new starting parameter of etch-track kinetics is given in Fig.4. It is clear from here that the actual value of h_c as a function of the incident angle and the "starting range", R_o, of the nuclear particle can be obtained from the solution of the equation

$$V(R_o - x_c)\sin\theta - 1 = 0 \qquad (7)$$

for $x_c = h_c/\sin\theta$. Taking into account eqs. (2) and (3) as etch-rate ratio vs residual range curves, from eq. (7) we can get

$$h_c = \sin\theta \left\{ R_o - \frac{1}{A} \ln \frac{\sin\theta}{1-\sin\theta} - \frac{B}{A} \right\} \qquad (8)$$

and

$$h_c = \sin\theta \left[R_o - \left(\frac{A\sin\theta}{1 - \sin\theta} \right)^{1/B} \right] \qquad (9)$$

From these it can be well seen that in practice we can meet with two cases, when $h_c = 0$ and when $h_c \neq 0$, respectively. In the first case the etched track formation starts immediately, in the second case only after a sufficiently long period of etching. The origin of the coordinate system used for describing the basic relations of etch-track kinetics is obviously to be placed in the $x_c = h_c/\sin\theta$ point of the particle trajectory (see Fig.4) for the case $h_c \neq 0$.

In order to demonstrate, in a realistic practical case, the importance of the above-mentioned parameter and the order of the delay of etch-pit formation, we have analysed track appearance for various light nuclei in Lexan. Our calculation was based on the procedure published in [8] for REL and range determination, starting from the

response function

$$V = 1 + 0.027\ REL^{2.84}, \qquad (10)$$

where the REL value is expressed in $MEVcm^2mg^{-1}$. As a result we got the curves indicated in Fig.5 which clearly show a sharp variation of the critical etching time, $t_c = h_c/V_B$, as a function of the specific energy and incident angle. The variation is so sharp that it may be usefully proposed as an identification method for ions entering the detector at appropriately tilted angles. It is interesting to note that the so-called etch induction time method proposed by Ruddy et al. [12], in experimental consequences appears to be very similar to the critical etching time method proposed by us here. The physical explanation of the origin of the two methods, however, is almost certainly different, since our h_c calculations for the CN foil used by Ruddy et al. have completely failed to explain their observations.

4. ETCH-TRACK FORMATION IN THICK ISOTROPIC SOLIDS AT CONSTANT ETCH-RATE RATIO

Let us consider now the etch-track kinetics for an isotropic track detector, assuming a constant etch-rate ratio. The basic idea of one of the most elegant mathematical treatments of this problem can be found in [13]. Other important details related to the track geometry of this case have been published in [2,3,6]. In this review I will first outline a simple demonstrative model of track

evolution, which in principle, is capable of describing completely our problem, and the formalism of which can be generalized and extended to the complete description of the etch-track kinetics for varying etch-rate ratios, too [5].

The Geometrical Model

When the chemical dissolution proceeds with a velocity V_T along a narrow central track region and with V_B velocity in other directions in the detector medium, mathematically the track shape can be considered as a "normal cone". The surface of this cone can be generated by the rotation of a straight line given by the equation

$$y=-x\,tg\delta+ L\,tg\delta, \quad \text{with } tg\delta= \frac{1}{(V^2-1)^{1/2}}, \; L=Vh, \qquad (11)$$

around the x axis of the coordinate system indicated in Fig.6. The equation of the circular conical surface can obviously be obtained from eq.(11) by replacing y by $(y^2+z^2)^{1/2}$. Thus, we have the relation

$$z^2 + y^2 - \frac{(x-hV)^2}{V^2-1} = 0 \qquad (12)$$

which describes the kinetics of track growth in the first so-called "cone phase" of etch-pit formation illustrated in Fig.6.

After a layer removal $h = R_o/V$, where R_o is the range of a nuclear particle, there is no more preferential etching along the axis of the track cone. The end of the track cone, in this phase, becomes spherical i.e. the track is composed of a conical and a spherical portion. It is a "partial cone

and sphere phase" of etch-pit formation, which may shortly be called "transition phase". The equation

$$z^2 + y^2 + (x-R_o)^2 - (h - \frac{R_o}{V})^2 = 0 \qquad (13)$$

represents the gradually growing sphere joined to the gradually diminishing cone portion in this phase.

Finally, in the last so-called "sphere phase" of etch-pit formation, the track becomes entirely spherical, when with the etched-off surface given by the equation

$$x - y\mathrm{ctg}\Theta - \frac{h}{\sin\Theta} = 0, \qquad (14)$$

the conical track portion is entirely removed.

Calculation of Track Parameters

With the knowledge of not more than four parameters (in our case V, Θ, h and R_o) and by using eqs. (12), (13) and (14) related to the track cone, track sphere and post--etch detector surface, one can quantitatively predict the variations of any track parameter during the chemical etching process.

The track profile is obviously given by eq. (11). The contour of the surface opening of the track can be obtained from the solution of the equations describing the track wall and detector plane. For the "cone phase" of track formation, for example, the solution is an ellipse defined by the equation

$$\frac{z^2}{a^2} + \frac{(y_o - \Delta y_o)^2}{b^2} = 1 , \qquad (15)$$

where a and b are the semiminor and respectively the semimajor axes of the ellipse and Δy_o is the "shift" of the point of intersection of the track cone axis with respect to the geometrical centre of the ellipse. The actual values of a, b and Δy_o are indicated in Fig.6. We note that at this calculation we used the $y = y_o \sin\Theta$ transformation, taking into account that the plane of the surface track contour is parallel with the plane determined by the z and y_o axes. This tranformation means that the track contour is replaced to the plane of the z and y_o axes.

In principle, similarly to the above procedure, from the solution of eqs. (13) and (14), one can get the track contour in the "sphere phase" of track formation. It is a circle determined by

$$z^2 + (y_o - \delta y_o)^2 = (h - \frac{R_o}{V})^2 - (h - R_o \sin\Theta)^2 = r^2, \quad (16)$$

where $\delta y_o = - \frac{h - R_o \sin\Theta}{tg\Theta}$.

With the equations (15) and (16) of the elliptical and circular parts of the surface track opening, the relations describing the evolution of the minor and major track axes are fully determined. From the point of view of track axes the phases of evolution indicated in Fig.7 can be distinguished. Two evolution phases exist for the minor axis but three phases for the major one. There is no need to explain the reason because the schematic drawing in Table I speaks for itself. Finally, it can be clearly

seen that the actual value of the track axes can be deduced from the relations

$$d_1 = 2a \ , \ d_2 = 2r \ ,$$
$$D_1 = 2b \ , \ D_2 = b + |\Delta y_c| + r - |\delta y_o| \ , \ D_3 = 2r \ , \tag{17}$$

and the h values at the phase boundaries of track evolution can be obtained from the solution of equations

$$\begin{aligned} \Delta y_o &= \delta y_o && \text{for } h = h_1 \\ b &= r + |\Delta y_o - \delta y_o| && \text{for } h = H_1 \\ b &= r - |\Delta y_o - \delta y_o| && \text{for } h = H_2 . \end{aligned} \tag{18}$$

For a better survey, the above track quantities are summarized in Table I.

5. ETCH-TRACK FORMATION IN THICK ISOTROPIC SOLIDS AT VARYING ETCH-RATE RATIO

There are several practical cases when the deviations from a perfect conical track shape are not negligible and the previously presented track formation model represents only a very rough approximation. Therefore, we must face a more complicated question i.e. how the track geometry can be described at a varying etch-rate ratio [1,3,4,5].

The Geometrical Model

Let us suppose that the track-etch rate is a monotonically changing function of the residual range of the nuclear particle in an isotropic solid (see e.g. Fig.3). In this case let us try to describe the etch-track growth in a form which allows the calculation of any track parameter of interest (pit-wall, track length, profile, axes,

contour) for nuclear particles entering the detector at arbitrary angles. If we want to avoid a sophisticated and complicated treatment of the problem without the loss of generality, it is advisable to try to find the simplest mathematical formalism possible. This requirement may be satisfied with a certain generalization of the geometrical model used previously for describing the different track evolution phases at a constant etch-rate ratio. We have to take into consideration, however, that at varying etch-rate ratios, under certain conditions, one more phase, the "incubation phase" of track evolution due to the existence of a critical layer removal, may appear (see eqs. (8) and (9)). One can also meet here the "cone", "transition" and "sphere" phases, but in the "cone phase" we actually have a track with a more complicated surface of revolution (see Fig.8).

A further distinction comes from the fact that the track shape shows a dependence on etch direction as compared to the direction of particle travel, as it is clearly shown by the photographs of alpha-track profiles in Fig.8 obtained in CR-39 polymer with the "track in track" method. The direction effect is schematically illustrated in Fig.9 from which one can clearly realize the analogy of track formation to an accelerating (forward track) or a slowing-down (backward track) wave source. This demonstrative picture can be usefully applied to the required simple description of the equation of the etch-pit wall at a varying etch-rate ratio.

A convenient coordinate system introduced into our problem is shown in Fig.10, in relation with a spatial picture of a forward track developing parallel with the travel direction of the particle. The origin of the system is fixed at the intersection of the original detector plane and the trajectory of the particle, so that the x axis should coincidence with the track axis. The y axis of the coordinate system lies in the plane determined by the particle trajectory and the direction of the major track axis. Using this system, the basic formulas describing etch-track kinetics consist of the equation of the etch-pit wall and that of the planes parallel with the detector surface. From the common solution of these equations, at a particular value of a parameter C introduced to determine the spatial position of the planes. one can answer all the questions of track evolution at a varying etch-rate ratio.

The etch-pit wall. In order to get the equation of the etch-pit wall, a realistic basic assumption must first be set up for the mechanism of etch-track formation. As it is suggested by Fig.8 and Fig.9, from the mathematical point of view the description of the evolution of an etch-pit wall is equivalent to the description of the evolution of a head wave produced by an object moving at a variable speed $V_T(x)$, in a medium having a wave propagation speed V_B. On the analogy of wave front production by a small object, the enhanced chemical dissolution of the material in a track is gradually delayed and is limited only to a narrow central zone of the

particle trajectory. At a given x_o coordinate point of the trajectory, the chemical dissolution of the bulk material starts after a delay

$$t(x_o) = \frac{h_c}{V_B} + \int_{x_c}^{x_o} V_T^{-1}(x)\,dx = \frac{h_c}{V_B} + \frac{H(x_o)}{V_B} \qquad (19)$$

and after that it takes place at a rate V_B along a spherical surface of increasing radii of

$$r(x_o) = V_B(t-t(x_o)) = h-h_c-H(x_o)\,, \qquad (20)$$

where t is the total etching time. In this way the equation of the surface of the spheres of bulk material dissolution can be given by

$$B(x_o) = z^2 + y^2 + (x-x_o)^2 - (h-h_c-H(x_o))^2 = 0. \qquad (21)$$

The etch-pit wall in this phase of track evolution can be considered as an enveloping surface of the family of $B(x_o)$ spheres, and is determined by the set of parametric equations

$$B(x_o) = 0\,, \quad \frac{\partial B}{\partial x_o} = 0\,, \qquad (22)$$

where $$\frac{\partial B}{\partial x_o} = x - x_o - (h - h_c - H(x_o))V^{-1}(x_o). \qquad (23)$$

This set of equations, which will shortly be referred to as the relation of "travelling balls" [5], describes the track growth in the "cone phase" of track formation.

As soon as etching has reached the end of a damaged particle trail of length R_o, after a layer removal $h = H(R_o)$ (see in Table II), there is no more preferential etching

and the track end becomes spherical. In this "transition phase" of track evolution, the formula

$$B(R_o) = z^2 + y^2 + (x-R_o)^2 - (h-h_c-H(R_o))^2 = 0, \quad (24)$$

derived from eq. (21) through the $x_o = x_{omax}=R_o$ substitution, represents the gradually growing sphere joined to the gradually diminishing "cone" portion. (The "cone" is only a conveniently short notation here, the real track is, of course, a more complicated body of revolution.) The formula (24) may be shortly called the "standing balls" relation.

In the last, "sphere phase" of track evolution the the "standing balls" relation is valid.

Planes parallel with the detector surface. In order to determine completely all the details of track formation at a varying etch-rate ratio, in addition to the "travelling and standing balls" relations, one should also determine the "moving planes" relation, i.e. the equation of the family of planes parallel with the detector surface (see Fig.10). A plane which intercepts, on the coordinate axes, the (nonzero) segments α, β, γ, can be represented by the equation

$$\frac{x}{\alpha} + \frac{y}{\beta} + \frac{z}{\gamma} = 1 \quad . \quad (25)$$

In our case, as can be seen from Fig.10, we have

$$\alpha = \frac{h + C}{\sin\Theta}, \qquad \beta = \frac{h + C}{\sin\Theta}\, tg\Theta, \qquad \gamma = \infty \quad . \quad (26)$$

Substituting these values into eq. (25), we obtain the equation of "moving planes" in the form

$$x - y\mathrm{ctg}\theta - \frac{h + C}{\sin\theta} = 0 \ . \qquad (27)$$

Calculation of Track Parameters

By using the eqs. (22), (24) and (27) one can quantitatively predict the evolution of any track parameter at a varying etch-rate ratio, on the full analogy of the methods used previously at a constant etch-rate ratio. Here, however, the common solution of the equations of "moving planes" and "travelling balls" cannot explicitly be given due to the complex parametric form of the latter one. Consequently, the relations with respect to the track parameters of interest can also be generally expressed in parametric form and their actual computation can be performed with successive iteration procedures.

Some of the formulas related to different track parameters are summarized in Table II. For simplicity, they are presented for the case $h_c = 0$. As concerns further details of practical calculations using these formulas one should refer to the work [8].

Finally, it is perhaps reasonable to present here the only case for which the track parameter calculation can be explicitly carried out. It must obviously be the situation of the "sphere phase" of track evolution where the formulas (24) and (27) to be used are not in parametric form. Using the condition $C = 0$ and the $y = y_o \sin\theta$ transfor-

mation, the solution of eqs. (24) and (27) can be expressed in the form

$$z^2 + (y - \delta y_o)^2 = (d/2)^2 \qquad (28)$$

where $\delta y_o = - \dfrac{h - R_o \sin\theta}{tg\theta}$, similarly to eq. (16), and the track diameter is given by

$$(d/2)^2 = (h-H(R_o))^2 - (h-R_o\sin\theta)^2 =$$
$$= [R_o\sin\theta - H(R_o)][2h - R_o\sin\theta - H(R_o)]. \qquad (29)$$

6. ETCH-TRACK FORMATION IN THICK UNISOTROPIC SOLIDS

Lastly, we must touch upon the etch-track kinetics for thick solids at an unisotropic bulk etching rate (see Fig. 2). I intend to deal with this question only very briefly because this situation cannot be treated as yet with the same generality and certainty as track evolution in an isotropic solid. In other words, at present, no etch-track formation model exists which would be valid for arbitrarily chosen unisotropic solids in the case of particles entering various crystallographic planes at arbitrary incident angles. In spite of the fact that valuable experimental data have been recently collected for the different etching properties and etch-pit formation characteristics of crystals [e.g. 1, 10, 14-19], there is so far no appropriate basis available to build up an appropriately general etch-track formation theory for unisotropic solids.

I can try to outline here some of the cardinal points that should come into consideration at a future theoretical description of etch-pit formation in crystals. At the same time, I emphasize that these effects should be the objectives of more detailed experimental studies in the future.

a) In crystals the track etch rate is also a varying quantity along the track. In most cases, however, it does not show such a smooth function as in amorphous solids [10]

b) Both the bulk and track etch rates display dependence on the crystallographic orientations. Consequently, the track appearance (critical angle for revealing tracks) as well as the various observable track parameters show more or less unisotropy in different directions in a crystal (e.g. [17] [19], Figs.11 c, d).

c) It appears that the shape of etch-pit figures, in certain cases, is influenced by the damage density along the track. This effect may be of special importance at small damages where the discontinuous damage distribution may result in serious consequences in etch-pit evolution.

d) The geometrical shape of track opening may also depend on the etching time (see e.g. [16]).

e) The etch-pit contour, is sometimes turned away at different depths of the track and even the shape of the contour may be changed in the same etch-pit at the same etching time.

f) The track wall frequently has a well-visible step-like structure (Fig.11d).

In the light (or shadow?) of the above considerations I am afraid to propose here any kind of definite track formation model for unisotropic solids. I shall consider only a simplified model [3] which, nevertheless, I hope, can fairly elucidate the essential differences between etch-pit evolution in isotropic and unisotropic solids. In crystals, according to this model, etch-pit formation is governed by three different etch rates. These are the track etch rate along the damage trail, V_T, the bulk etch rate in a direction normal to the surface plane of the crystal, V_B, and the bulk etch rate parallel to the surface plane, V_p, where V_P is a function of crystal surface orientation. Assuming a constant V_T along the track, the expectable track profile in a given plane of symmetry seems to be the one illustrated in Fig.12. Here, from the point of view of track axis evolution, two phases are to be distinguished in which the axes can be given by the relations

$$d_1 = 2h \frac{V_P}{V_B} \left(1 - \frac{V_B}{V_T \sin\Theta} \right), \quad 0 \leq h \leq h_1 = R_o \sin\Theta \qquad (30)$$

$$d_2 = 2R_o \sin\Theta \frac{V_P}{V_B} \left(1 - \frac{V_B}{V_T \sin\Theta} \right), \quad h_1 \leq h \ . \qquad (31)$$

In addition, the angles at the track tip in the two phases can be calculated from

$$\operatorname{tg} \delta_1 = \frac{2\sin\Theta \, (V_T/V_P)}{(V_T/V_P)^2 - 1} , \tag{32}$$

$$\operatorname{tg} \frac{\delta_2}{2} = V_P/V_B . \tag{33}$$

The above equations fairly represent the main features of track evolution in crystals. For example if $V_B \approx 0$ and $V_T >> V_P$, we have a track generally observable in muscovite and phlogopite micas, i.e. $\delta_1 \approx 0^o$, $\delta_2 \approx 180^o$ and d_1 is a linear function of etching time (from eq. (30) $d_1 = 2V_p t$).

7. SELECTED THEORETICAL AND PRACTICAL QUESTIONS

Henceforward, in the knowledge of the basic information on etch-track kinetics in solid state nuclear track detectors, we can direct our attention to the question how we can apply this theory in practice and how we can get useful information by using it. This is, of course, a very branching-out question and we must confine ourselves here only to a few selected problems. First, I want to say a few words about some methods for determining unknown track parameters, then I want to show some results related to surface track sizes calculated with the theoretical formalism presented here, and finally I wish to present the way how we can solve the problem of etch-hole formation in thin isotropic foils.

Methods for Determining Unknow Track Parameters

Up to this point we have used only four selected parameters (h, θ, R_o, V) to describe etch-track kinetics. In different practical situations, however, these parameters must be replaced by other ones. The best set of parameters should obviously be chosen for each particular situation, depending on the calculation requirements and measurement facilities. It is clear that for this purpose the knowledge of the relations supplying the connection between the unknown and measurable (or known) track parameters is greatly required. Such relations would also be very useful in the cases when the parameters of interest are obtained from procedures of fitting the theoretical and experimental results.

Some of the most useful relations derived and applied by myself [3] and other [1,2] for different etch-track situations in isotropic solids are summed up in Table III. I don't want to comment on these relations one after the other, because most of them are self-evident or easily understandable from the illustrative figures attached to the Table. I prefer to select only one relation for each track parameter (angle of incidence, cone angle, track length, etch-rate ratio) included in the Table.

One of the most useful relations for determining the angle of incidence in case of an unknown track is eq.2' in table III, derived from the equations d_1 and D_1 in Table I . Its use requires the knowledge of the well-measurable minor and major track axes and the extent of

layer removal. The latter one can also be obtained from the minor track axes related to fission fragment tracks ($2h \approx d_f$ for not to small Θ). According to our experience the angle data calculated from eq.2' agree extremely well with the expected values for both long and short-range tracks. It should be noted, however, that this equation holds only for certain, not too high values of layer removal, and only in the "cone phase" of etch-track formation (see Fig.11a).

The value of the cone angle of a track can be generally determined from the simple relation

$$\sin \delta = \cos\Theta . \sin \delta_p , \qquad (34)$$

if the angle of incidence is known and the projected cone angle, δ_p, can be well measured on the surface of the detector. Otherwise, the eq.3' in Table III can be usefully applied.

The relation of real track length to other track parameters is frequently required. This demand arises particularly in studies concerned with particle identification based on the well-known L(R), track length-residual range method. For longer track cones the conventional relation represented by eq.4' can be naturally applied. For shorter tracks, however, it fails to work and one should choose track parameters measurable in the horizontal plane of the detector. For such a situation a useful relation may be, for example, the one given by eq.6' in Table III together with eq.2', which can be applied, in the "cone phase" of track formation. It should be noted that track lengths (ranges) can be determined even in the "sphere phase" of

track formation for very shallow etch-pits, too (see Fig.11b). For this situation a method based on eq.(29) was published in [3].

Finally, few words should be devoted to the determination of the etch-rate ratio, one of the most important parameters of etch-track kinetics. Generally one can say that this parameter is advisable to derive from track lengths at high radiation damages and, respectively, from track axes at low damages, but in both cases at reasonably small layer removal. Here, I prefer to emphasize the still less-known track axis method represented by eq.8' in Table III. According to our experience it can be reliably used even for rather oblique track cones. The etch-rate ratio, however, with fair approximation, should be related to the residual range $R = R_o - h/\sin\theta$.

Calculation of Surface Track Sizes

Let me continue my talk by presenting some actual etch-track calculations for both constant and varying etch-rate ratios, performed by using the etch-track formation model discussed previously. From among the numerous possibilities allow me to choose only one with which I am particularly familiar, the problem of surface track size calculations. This field is very suitable, to demonstrate the possibilities involved within the theory and the usefulness of calculations before performing time-consuming experiments. From our examples it also becomes clear that track calculations are greatly needed to ensure the proper

interpretation of different track measurements.

As a first example, in Figs. (13) and (14), we show a typical set of theoretical curves illustrating the variation of the minor and major track axes as a function of layer removal at different incident angles. The curves were calculated at a particular value of V and R_o characteristic of fission tracks in soda glass by using the relations of the track size evolution phases given in Table I. One can clearly see that the evolution of the minor and major track axes is strongly different in character. From the practical point of view, the d_1 and D_1 evolution phases are particularly interesting, in which the relations summed up in Table III are valid. The minimum values of layer removal characteristic of these phases can obviously be obtained if Θ is replaced by $\Theta_c = \arcsin V^{-1}$ in the formulas d_1 and D_1. Thus, we have

$$d_1(\Theta_c) = 0\,, \qquad h_1(\Theta_c) = 2R_o/V\,, \tag{35}$$

$$D_1(\Theta_c) = R_o\sqrt{1 - V^{-2}}\,, \qquad H_1(\Theta_c) = R_o/V. \tag{36}$$

From this one can see that if $h \leq R_o/V$ the relations describing the evolution of the minor and major axes are definitely valid at any incident angles, i.e. for tracks obtained in an irradiation in 2π-geometry.

As a second illustrative example we choose the calculation of the theoretically expectable variation of the track diameter of different light nuclei as a function of their "starting" range at particular thicknesses of layer removal. For the actual calculations the change of the etch-rate ratio along the residual range of the particles

was described by the empirically obtained functions given in [5] for a polycarbonate detector. The curves calculated for $\theta = 90^{o}$ are presented in Figs. 15 and 16. From Fig.15 one can see that polycarbonate, one of the least-sensitive alpha-track detectors (see Fig.3) has proved to be one of the best detectors in alpha-particle spectrometry as a consequence of the high sensitivity of the track size to alpha-particle energy. This behaviour offers useful practical application possibilities especially in nuclear reaction studies [20]. Maximum energy resolution can be attained at the inflexion points of the curves (dotted line in Fig.15). It can also be seen that the range resolution reaches saturation (i.e $\Delta d/\Delta R = const$) at above 3 MeV. Such calculations can obviously be extended to other detector materials, too. Thus, e.g. one can explain all the properties of the experimental curves obtained for various glasses as energy detectors for fission fragments [21,22].

The calculated curves shown in Fig.16 indicate that with extended etching in polycarbonate a fairly good energy and charge resolution can also be attained for various, normally incident light nuclei. It is interesting to note here that the above sets of curves remain valid even for tracks of oblique incidence by using a so-called effective track diameter calculated from

$$d_{eff} = 2h\,(\sqrt{1 + C^2} - C), \quad C \equiv \frac{1-B^2}{2A} \qquad (37)$$

in the knowledge of the minor and major track axes in the

"cone phase" of track evolution ($A \equiv D/2h$, $B \equiv d/2h$). This transformation gives a new possibility to extend the use of the track-diameter method to particles incident at arbitrary angles on the detector surface.

As a third illustrative example we use the theory of etch-track evolution to predict the expectable variation of the surface track contour of alpha-tracks at different incident angles in the least and in the most sensitive alpha-track detector shown in Fig.3. The results given in Fig.17 were obtained by using a computing programme based on the "track contour formula" in Table II. The contours obtained clearly show the high effect of detector sensitivity on track appearance.

Etch-Hole Formation in Thin Foils

As a last discussion point of my talk I have chosen a quite complex set of problems related to the perforation and hole-formation process in thin isotropic foils. Although this set of problems is getting more and more important in different track applications (e.g. spark counting, radiography with double-layered or strippable films, nuclear filters), to the best of my knowledge, there is no comprehensive theory available in this field. In the last few years in our laboratory we have made efforts to solve this problem [23,24] by extending the theory of etch-track formation to the specific condition of thin foils. Here, without going into details, I wish to present some results of this study and at the same time to illustrate how complicated etch-hole formation can be at different initial conditions.

Foil perforation. The easier part of the problem is the determination of the moment of perforation (see e.g. in Fig.22d) as a function of the particle and detector parameters. A schematical illustration on the possible etching situations leading to the perforation of a thin film with (situation S) and without (situation T) support layer is given in Fig.18 for a constant etch-rate ratio, and in Fig.19 for a varying one. For these etching situations, the relations determining the "perforation layer removal", h_p, are summed up in Tables IV and V. If we use the relation $V(R) = 1+\exp[-0.205R\ (\mu m)+3]$ obtained for a stripped 13 μm thick strippable Kodak LR-115 film, one can get the curves indicated in Fig.20. (Details of calculation with a V(R) function of such form can be found in [24].) The calculated curves clearly show the sensitivity of the perforation of a thin foil to the ranges and incident angles of alpha-particles. From such calculations one can easily derive also the changes in the efficiency of track hole registration as a function of the residual thickness of the etched foil.

Pore size evolution. After foil perforation a much more complicated task is the description of the evaluation of the size of etched-through tracks (henceforth only pores, see e.g. in Fig.22c). From the practical point of view, regarding the perforated foil as a filter, the most interesting parameter may be the minor axis in the pore section of minimum area. The evolution of the minor hole axis in this pore section was determined for all the

possible etching situations S and T illustrated in Fig.18. The results obtained for a constant etch-rate ratio are shown in Table VI. The nine relations found to be necessary for a complete description of the problem indicate the wide variety of the cases for the production of a nuclear filter. A study of the practical consequences of these relations at various initial conditions is in progress in our laboratory.

Another, even more complex problem is the description of the evolution of pore size at a varying etch-rate ratio. This problem can also be completely solved by using the relations of etch-track kinetics, given in Table II. Here, for simplicity, I present results only for track holes related to nuclear particles incident normally to the surface of a stripping film. The formulas for describing the etch-hole diameters at the back and top surfaces of such a film are summarized in Table VII. (Note that here the S and T etching situations are denoted by small s and t letters to make distinction between the cases given in Table VI and Table VII.) These formulas were obtained by taking into account that for the top surface $C = 0$, for the back one $C = l_o - h$ and for both cases at $\theta = 90^o$ the equality $|y_1| = |y_2| = d/2$ are valid in the formulas in Table II.

According to our recent experience, the formulas given in Table VII. can be efficiently used for predicting the behaviour of tracks in different applications. As an illustration of this statement, in Fig.21, I present the result of

a track-hole calculation for alpha-particles of different energy, entering a 13 μm thick LR-115 strippable film at right angles. In the figure the etch-hole diameter is shown in the surface plane of the foil supporting the red-dyed cellulose nitrate layer. As can be well seen such a calculation predicts the best etching condition ($l_o - h \approx 9\text{-}10$ μm) for high-resolution alpha-radiography and at the same time clearly indicates the width of the energy interval in which brigth alpha-tracks (holes) can be observed. Such information can obviously be obtained experimentally only by performing very time-consuming measurements.

When I was invited to give this lecture, I thought it would be appropriate to speak first about the most important theoretical aspects of the evolution of etch-tracks under different initial conditions and then to demonstrate the possibility, the method and the results of certain typical applications of the theoretical considerations. I hope, I have achieved this aim in the necessary degree and all of you will make good use of this knowledge in your future studies in any phase of the evolution of your home tracks.

REFERENCES

[1] R.L. Fleischer, P.B.Price and R.M.Walker, Nuclear Tracks in Solids, University of California Press, Berkeley, 1975, Chap.2, pp.50-64.

[2] R.P.Henke and E.V.Benton, Nucl.Instr.Meth. 97, 483 (1971).

[3] G.Somogyi and S.A.Szalay, Nucl.Instr.Meth. 109,211 (1973).

[4] H.G.Paretzke, E.V.Benton and R.P.Henke, Nucl.Instr. Meth. 108, 73 (1973).

[5] G.Somogyi, R.Scherzer, K.Grabisch and W.Enge, Nucl. Instr.Meth. 147, 11 (1977).

[6] A.Ali and S.A.Durrani, Nucl. Track Detection 1, 107 (1977).

[7] G.Siegmon, H.J.Köhnen, K.P.Bartholomä and W. Enge, Rad. Effects 34, 9 (1977).

[8] G.Somogyi, K.Grabisch, R.Scherzer and W.Enge, Nucl. Instr. Meth. 134, 129 (1976).

[9] G.V. McKinley, Rad.Effects 37, 199 (1978).

[10] P.B.Price, D.Lal, A.S.Tamhane, and V.P.Perelygin, Earth Planet.Sci.Lett. 19, 377 (1973).

[11] B.G.Cartwright, E.K.Shirk and P.B.Price, Nucl.Instr. Meth. 153, 457 (1978).

[12] F.H.Ruddy, H.B.Knowles and G.E.Tripard, Phys.Rev.Lett. 37, 826 (1976).

[13] E.V.Benton, USNRDL-TR-68-14. U.S.Nav.Rad.Def.Lab., San Francisco, California, (1968) pp.60-69

[14] G.W.Dorling, R.K.Bull, S.A.Durrani, J.H.Fremlin and H.A.Khan, Rad. Effects, 23, 141 (1974)

[15] W.Krätschmer, Nucl.Instr. Meth. 147, 205 (1977)

[16] K.Thiel, H.Külzer and W.Herr, Nucl. Track Detection 2, 127 (1978)

[17] K.Thiel, H.Külzer, Rad.Effects 35, 87 (1978)

[18] P.F.Green, R.K.Bull and S.A.Durrani, Nucl.Instr.Meth. 157, 185 (1978)

[19] H.A.Khan and R.A.Akber, Proc. of the 9th Int. Conf. on Solid State Track Detectors, Pergamon Press, 403 (1978)

[20] G.Somogyi, I.Hunyadi, E.Koltay and L.Zolnai, Nucl.Instr. Meth. 147, 287 (1977)

[21] J.Aschenbach, G. Fiedler, H.Schreck-Köllner and G. Siegert, Nucl.Instr.Meth. 116, 389 (1974)

[22] V.A. Nikolajev and V.P.Perelygin, Pribory Techn. Exp. No.2, 7 (1976)

[23] Gy.Almási, Theory of nuclear filters and conductometric investigations of the filter parameters (In Hungarian), Competition work at the University of Kossuth L. in 1977 and 1978

[24] G.Somogyi and Gy.Almási, to be published

[25] G.Somogyi, L.Medveczky, I.Hunyadi and B.Nyakó, Nucl. Track Detection, 1, 131 (1977)

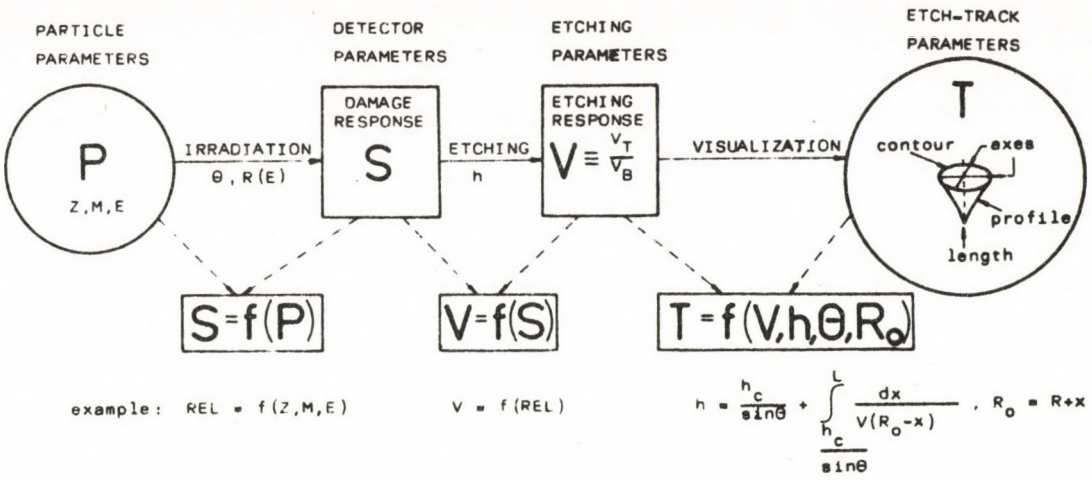

Fig.1 Schematic representation of the basic relations of the irradiation, track etching and track visualization phases.

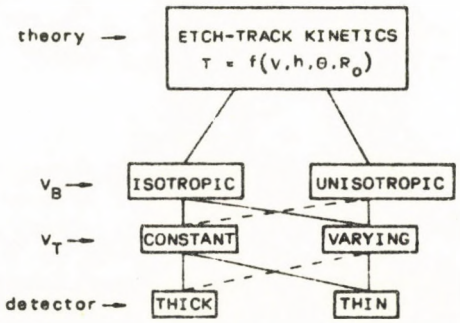

Fig.2 Etch-track kinetics classification according to the etching and detector properties.

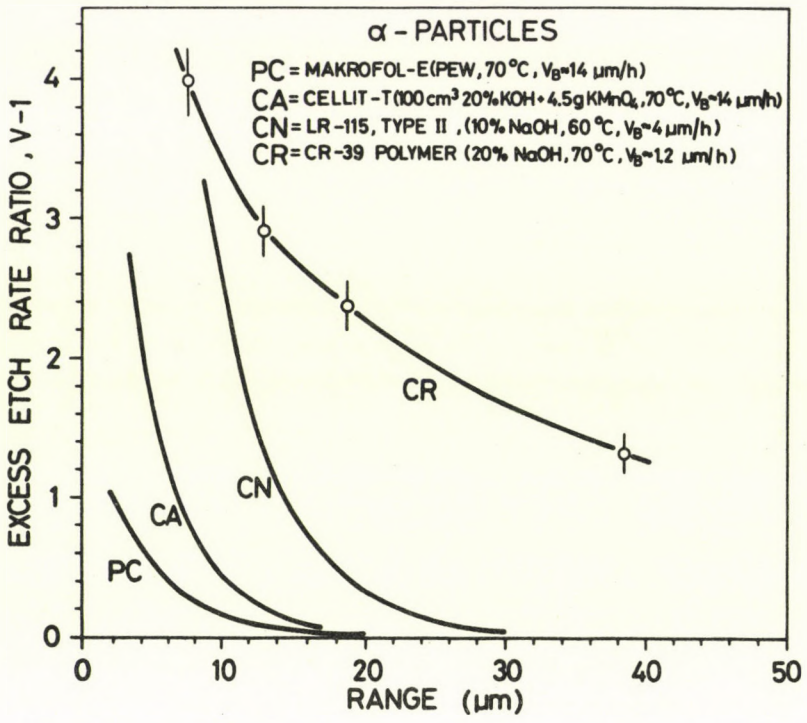

Fig.3 Excess etch-rate ratio as a function of the residual range of alpha--particles for various polymers.

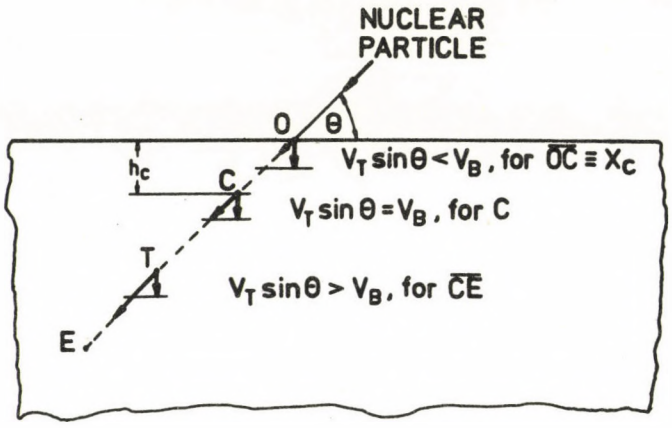

Fig.4 Schematic representation of the increase of track etch rate (V_T) in comparison with the bulk etch rate (V_B) along the damage trail of a charged nuclear particle.

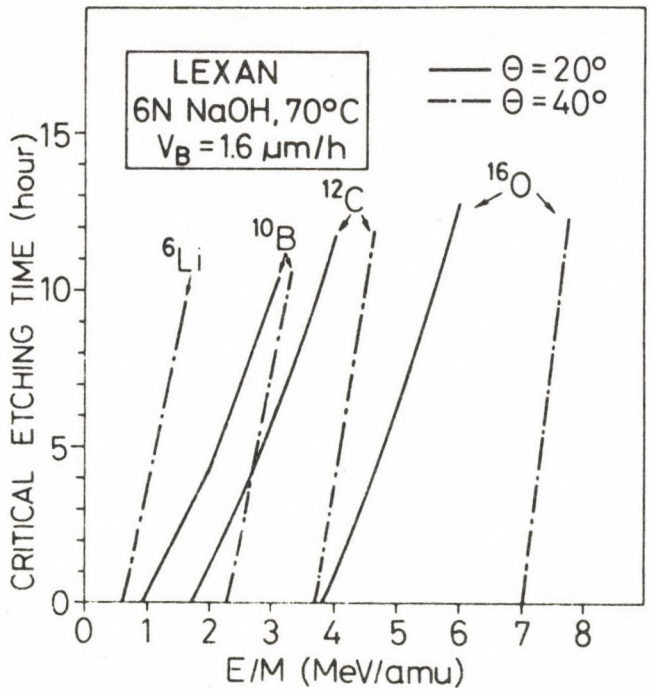

Fig.5 Critical etching time, $t_c = h_c/V_B$, for the first appearance of tracks of various light nuclei as a furction of their specific energy.

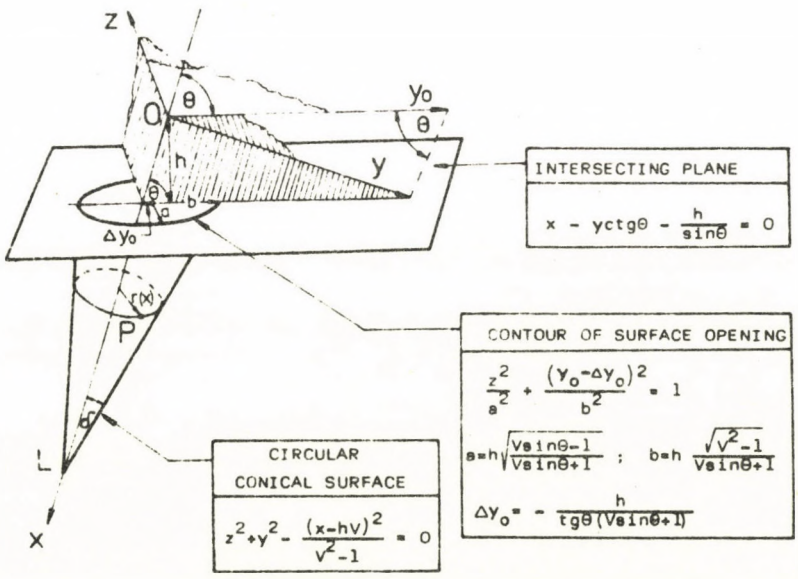

Fig.6 Scheme for describing etch-pit quantities in the "cone phase" of track formation in isotropic solids at a constant etch-rate ratio, V.

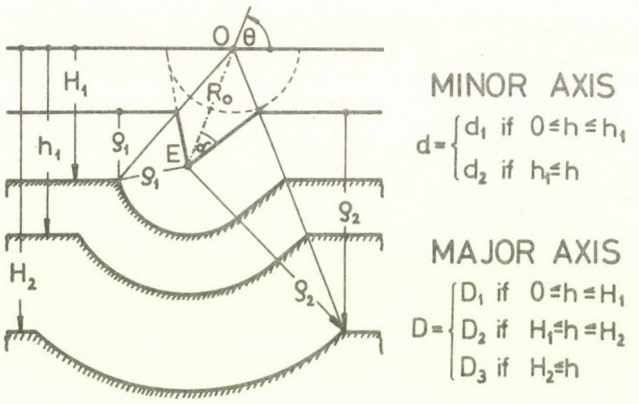

Fig.7 Typical phases and their validity range for describing track axis growth in isotropic solids at a constant etch-rate ratio.

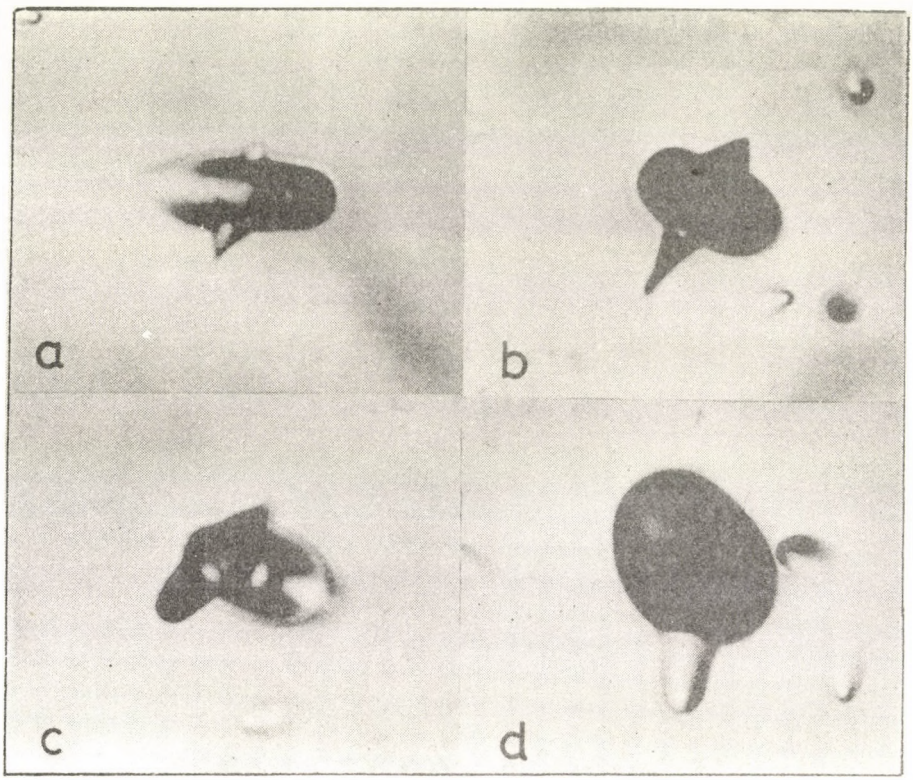

Fig.8 Examples of tracks showing typical profiles of forward and backward etch-pits. The photographs were taken of alpha-tracks in fission track observed in CR-39 polymer placed in contact with a ^{252}Cf source.

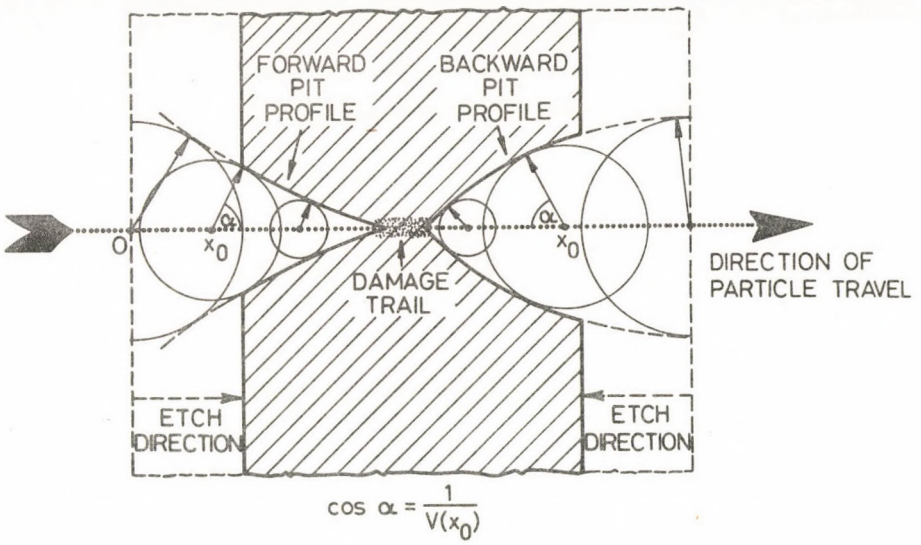

Fig.9 Schematic view of the formation of forward and backward etch-pits in an isotropic solid, i.e. when during etching the track tip develops parallel with and opposite to the direction of particle travel, respectively.

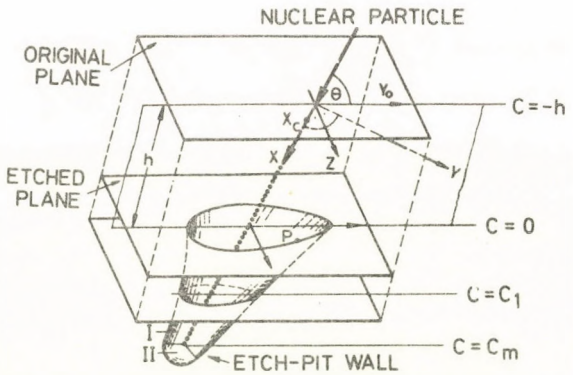

Fig.10 Scheme for describing etch-pit quantities in isotropic solids at a varying etch-rate ratio, $V(x_0)$, along the trajectory of a nuclear particle.

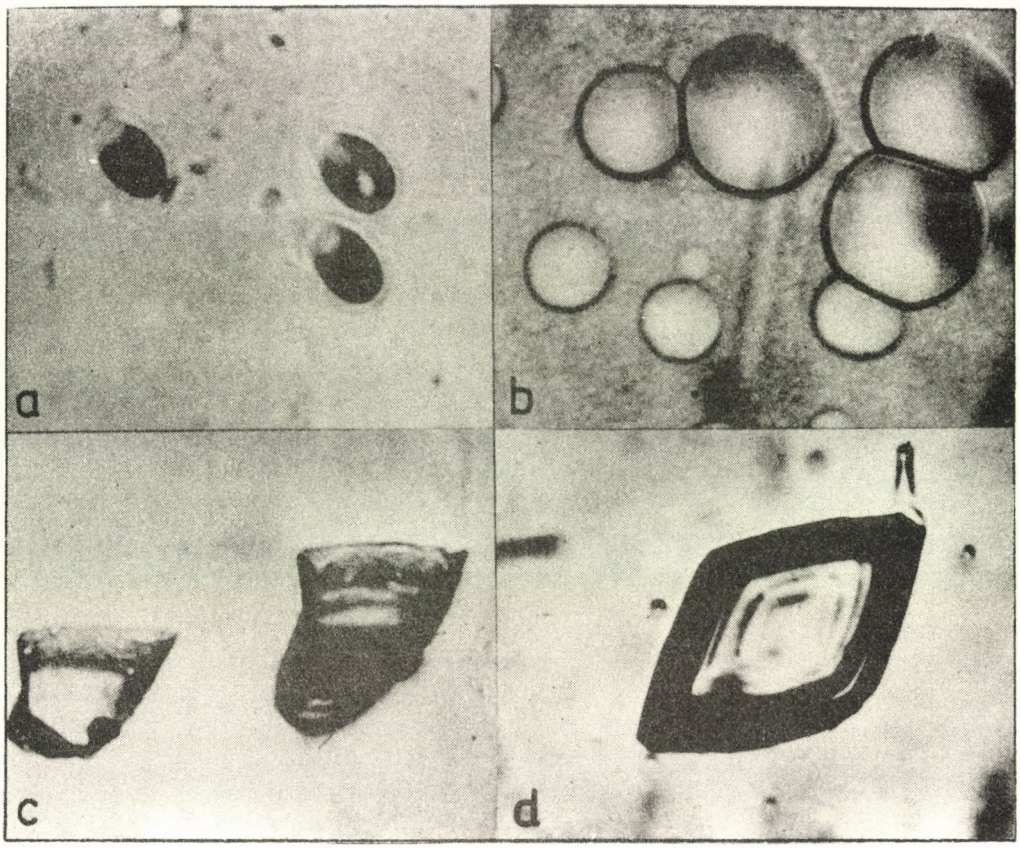

Fig.11 Examples of typical track contours a) alpha-tracks at 45° in PC ("cone phase"); b) fission tracks at 90° in glass after extended etching ("sphere phase"); c) fission tracks at 45° in biotite; d) fission track at 90° in muscovite

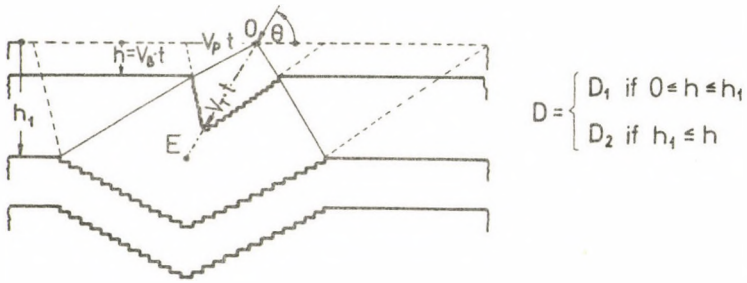

Fig.12 Schematical view of etch-pit formation phases in an unisotropic solid at constant etch-rate ratio

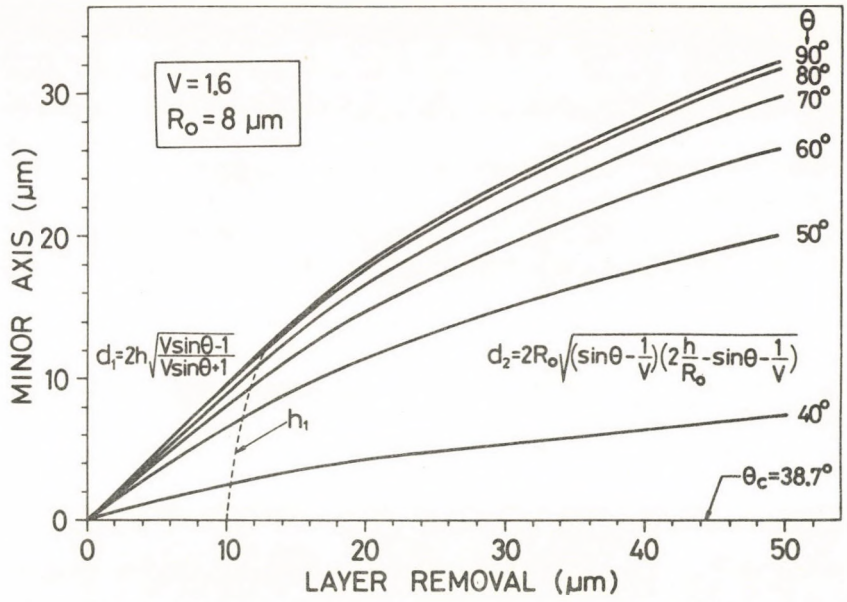

Fig.13 Theoretical curves showing the variation of minor track axis as a function of layer removal in the track formation phases, at different incident angles. The calculations were performed using the formulas in Table I.

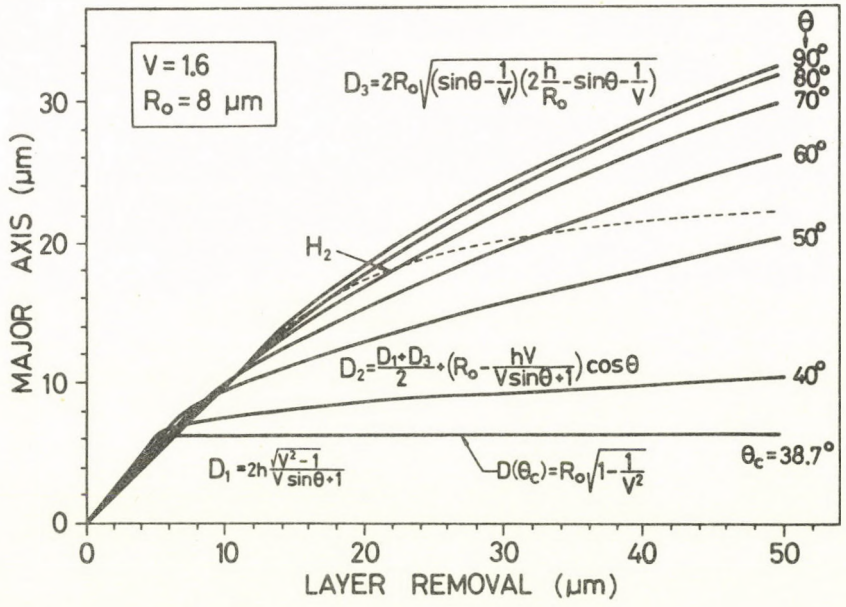

Fig.14 Theoretical curves showing the variation of major track axis as a function of layer removal in the track formation phases, at different incident angles. The calculations were performed using the formulas in Table I.

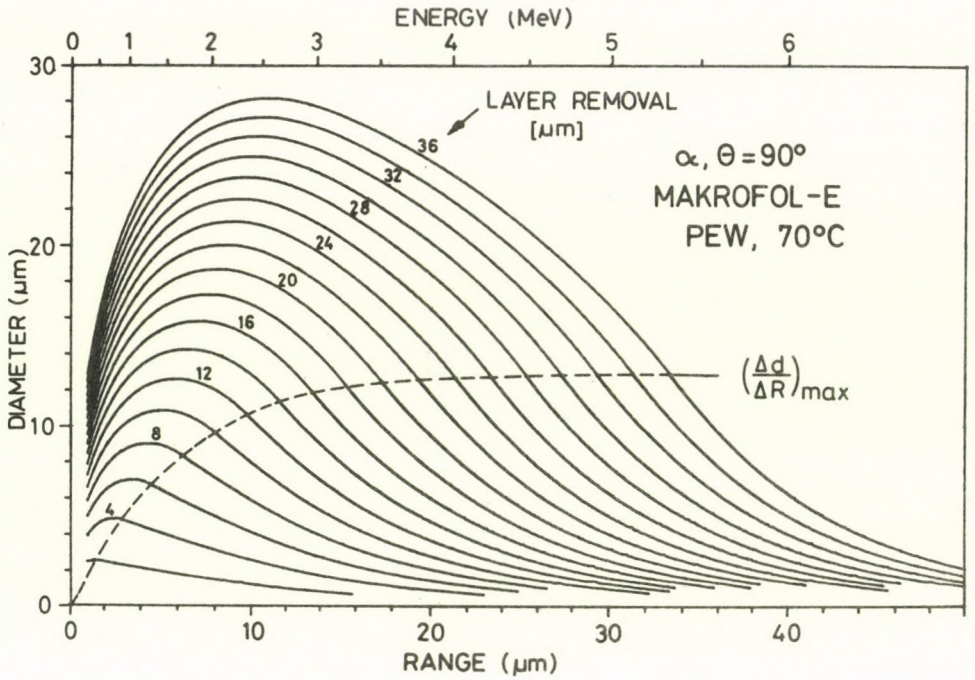

Fig.15 Theoretical curves showing the variation of the diameter of forward tracks as a function of the "starting" range (and energy) of normally incident alpha-particles in PC, at different degrees of layer removal.

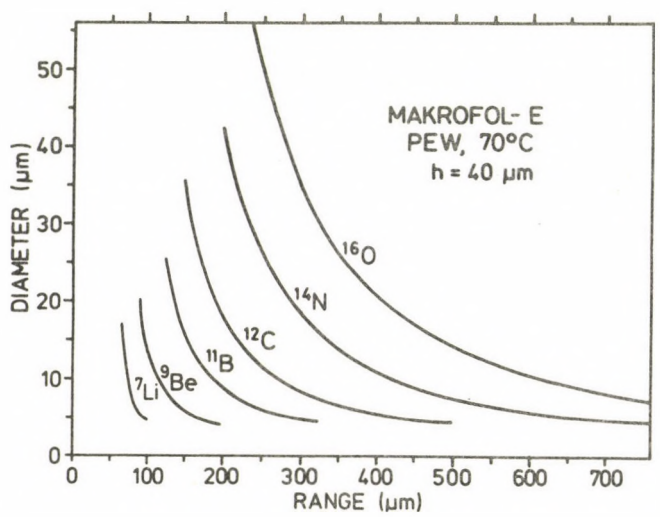

Fig.16 Theoretical curves showing the variation of the diameter of forward tracks as a function of the "starting" range of various light nuclei in PC, at extended etching.

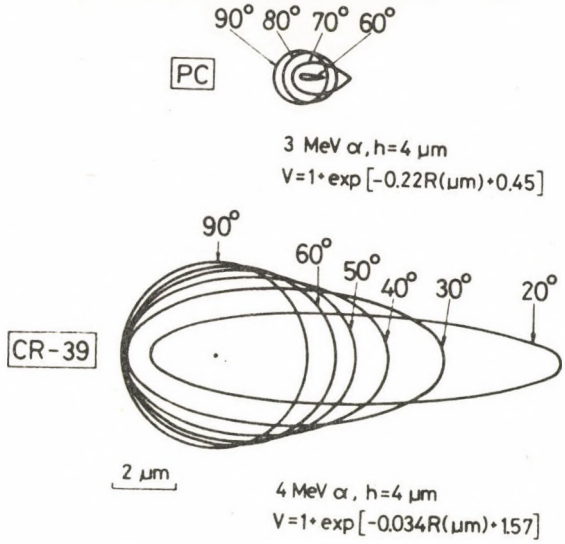

Fig.17 Calculated track contours for 3 MeV alpha-particles in PC and for 4 MeV alpha-particles in CR-39 polymer as a function of the incident angle. The calculations were performed using the experimentally derived V(R) functions indicated in the Figure.

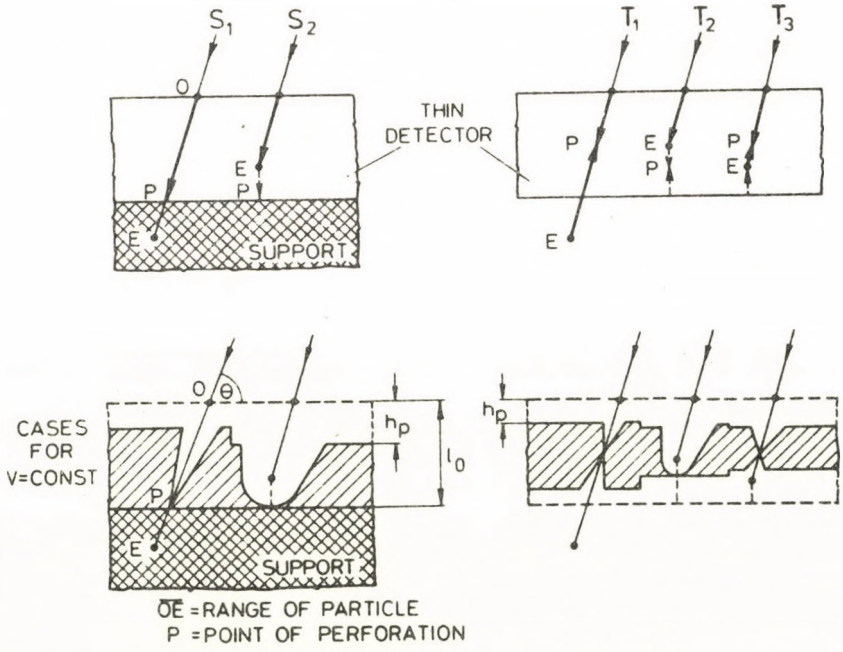

Fig.18 Schematic drawing of the etching situations leading to track perforation through a thin isotropic foil with (S) and without (T) support layer in case of a constant etch-rate ratio.

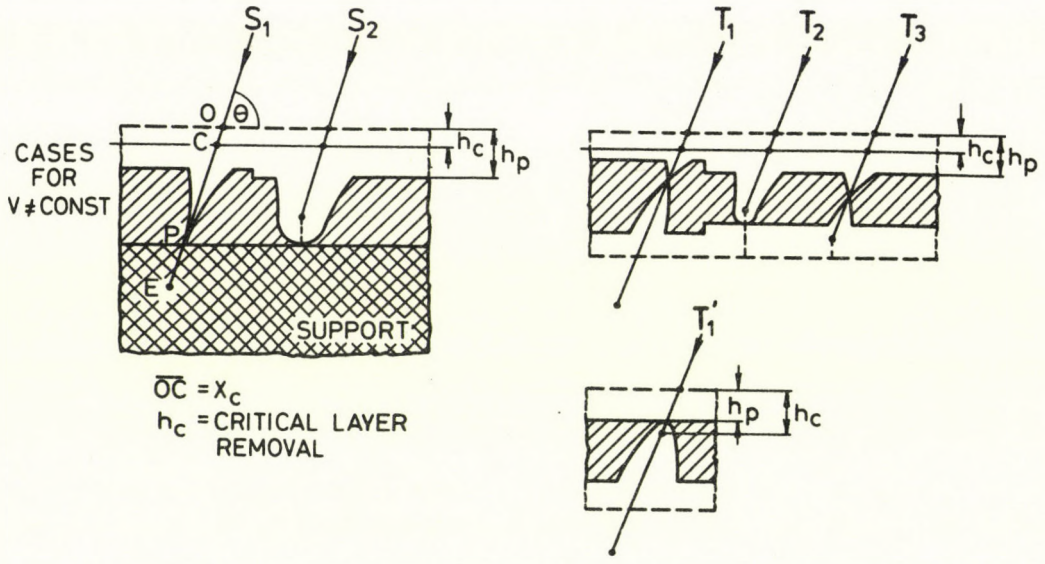

Fig.19 Schematic drawing of the etching situations leading to track perforation through a thin isotropic foil with (S) and without (T) support layer in case of a varying etch-rate ratio.

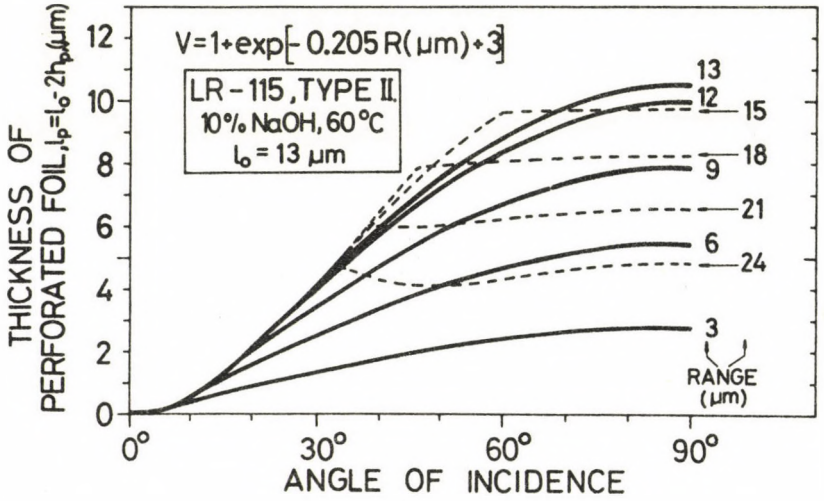

Fig.20 Calculated residual thickness of an etched-through CN foil without a support layer in the moment of perforation as a function of the angle of incidence of alpha--particles of various ranges.

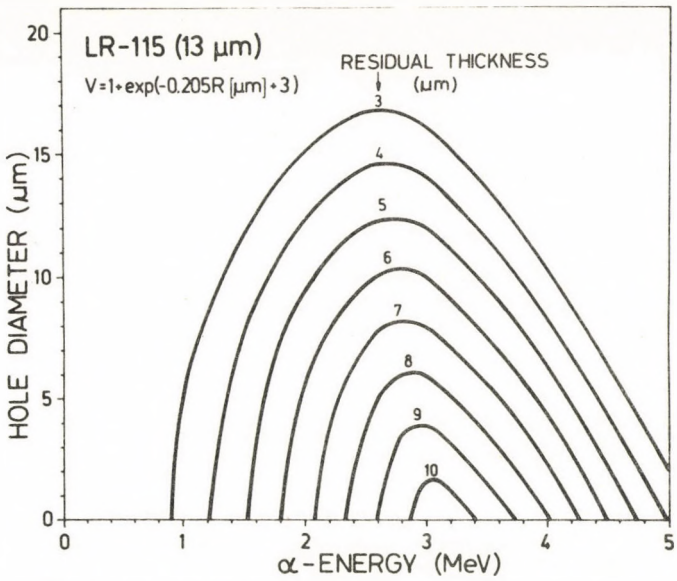

Fig.21 Calculated hole diameter in a stripping film (13 µm thick foil with support layer) as a function of alpha-particle range, at different residual thicknesses of foil.

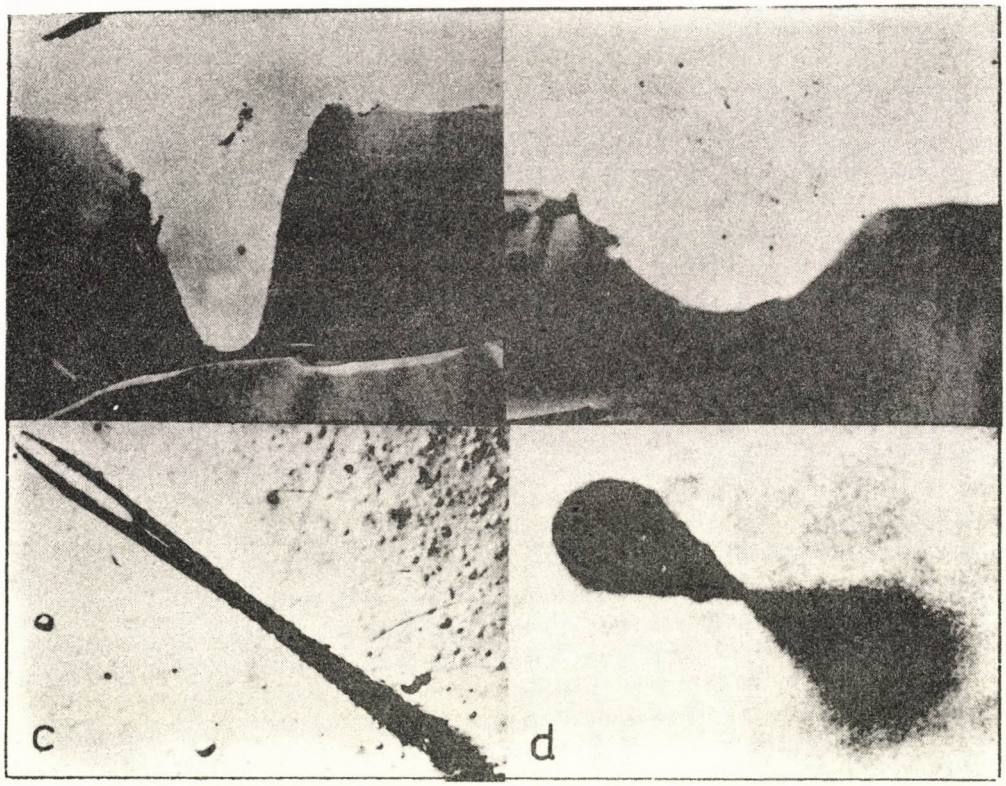

Fig.22 Examples of typical track profiles a) alpha-track in CA ("transition phase"); b) alpha-track in PC ("sphere phase"); c) heavy ion track in thin CN after perforation (etching situation T_1); d) heavy ion track in thin CN before perforation (etching situation T_1).

Table I. Formulas for describing track length and axes in thick isotropic solid at constant etch-rate ratio

	FORMULAS[+]	VALID IF[++]
TRACK LENGTH L	$L = Vh$	$0 \le h \le \frac{R_o}{V}$
MINOR TRACK AXIS d	$d_1 = 2h\sqrt{\frac{V\sin\theta - 1}{V\sin\theta + 1}}$ $d_2 = 2R_o\sqrt{(\sin\theta - \frac{1}{V})(2\frac{h}{R_o} - \sin\theta - \frac{1}{V})}$	$0 \le h \le h_1 = R_o(\sin\theta + \frac{1}{V})$ $h_1 \le h$
MAJOR TRACK AXIS[++] D	$D_1 = 2h\frac{\sqrt{V^2 - 1}}{V\sin\theta + 1}$ $D_2 = \frac{1}{2}(D_1 + D_3) + (R_o - \frac{hV}{V\sin\theta + 1})\cos\theta$ $D_3 = 2R_o\sqrt{(\sin\theta - \frac{1}{V})(2\frac{h}{R_o} - \sin\theta - \frac{1}{V})}$	$0 \le h \le H_1 \equiv R_o\frac{(V^2-1)\sin\theta + A}{V - \sin\theta + A}$ $H_1 \le h \le H_2 \equiv R_o\frac{(V^2-1)\sin\theta - A}{V - \sin\theta - A}$ $H_2 \le h$

+ h = layer removal from single surface of detector;
$V \equiv V_T/V_B$ = etch-rate ratio; R_o = etchable range of particle;
θ = angle of incidence of particle to the detector surface;
$\theta_c = \arcsin V^{-1} \le \theta \le 90^o$

++ $A \equiv \cos\theta\sqrt{V^2 - 1}$

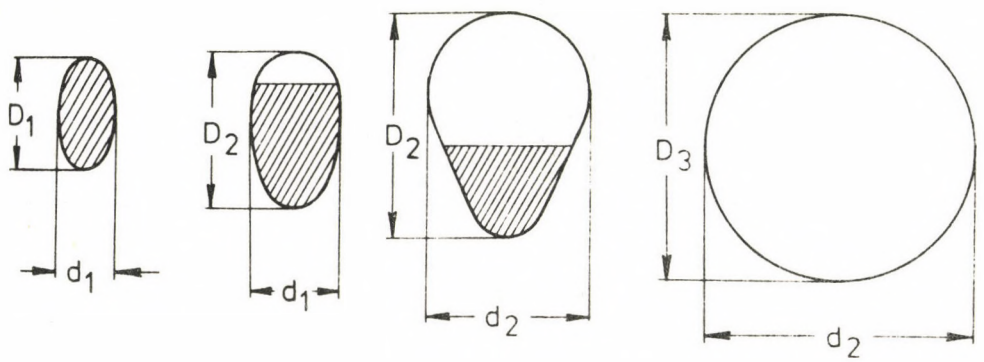

Table II. Formulas for describing etch-track parameters in thick isotropic solid at varying etch-rate ratio

		FORMULAS[+]	REMARK
PLANES PARALLEL WITH DETECTOR SURFACE		$x - y\mathrm{ctg}\theta - \frac{h + C}{\sin\theta} = 0$	
ETCH-PIT WALL	I	$(x-x_o)^2 + y^2 + z^2 - (h-H(x_o))^2 = 0$ $x-x_o - \frac{h - H(x_o)}{V(x_o)} = 0$	$H(x_o) \equiv \int_{x_c}^{x_o} V^{-1}(x)\,dx$ $H(R_o) \equiv H(x_o)\big\vert_{x_o=R_o}$ $x_c \leq x_o \leq R_o$
	II	$(x-R_o)^2 + y^2 + z^2 - (h-H(R_o))^2 = 0$	
TRACK LENGTH $L(h)$		$h = \int_{x_c}^{L} V^{-1}(x)\,dx$	
TRACK PROFILE $P(x, y_i)_h$		$y_i = w_i \frac{h - H(x_o)}{V(x_o)} \quad x = x_o + \frac{h - H(x_o)}{V(x_o)}$ $h = H(x_o) + \frac{x_o\sin\theta - H(x_o) - C}{1 - V^{-1}(x_o)(\sin\theta - W_i\cos\theta)}$	$w_i \equiv (-1)^i\sqrt{V^2(x_o) - 1}$ $i = 1,2$
MAJOR TRACK AXIS D		$D = \frac{\lvert y_1 - y_2\rvert}{\sin\theta} = \frac{\lvert y_1\rvert + \lvert y_2\rvert}{\sin\theta}$	if $C = 0$
TRACK CONTOUR $P\left(z, y_o = \frac{y}{\sin\theta}\right)_h$		$z = \pm\left[(h-H(x_o))^2 - y^2 - \left(y\mathrm{ctg}\theta + \frac{h+C}{\sin\theta} - x_o\right)^2\right]^{\frac{1}{2}}$ $h = H(x_o) + \frac{x_o\sin\theta - y\cos\theta - H(x_o) - C}{1 - V^{-1}(x_o)\sin\theta}$	$0 \leq C \leq R_o\sin\theta - h$

[+]If $x_c \neq 0$, in all the equations the transformation

$x_o \longrightarrow x_o - x_c$ and $h \longrightarrow h - h_c = h - x_c\sin\theta$

must be peformed

TableIII. Methods for determining unknown track parameters in terms of measurable (or known) track quantities in isotropic solid

TRACK PARAMETERS	Eq. No.	RELATIONS	Fig. No.
ANGLE OF INCIDENCE θ	1'	$\tan\theta = \frac{\Delta z}{\Delta x}$	①
	2'	$\sin\theta = \frac{1 + B^2}{\left[(1-B^2)^2 + 4A^2\right]^{1/2}}$; $B \equiv \frac{d}{2h}$; $A \equiv \frac{D}{2h}$;	②
CONE ANGLE δ	3'	$\sin\delta = V^{-1} = \frac{h}{L}$	②
REAL TRACK LENGTH L	4'	$L = \frac{z + h}{\sin\theta}$	③
	5'	$L = \frac{z}{\sin\theta - \sin\delta}$	③
	6'	$L = \frac{h + (p + \frac{D}{2} - \Delta y_o)\tan\theta}{\sin\theta}$; $\Delta y_o = h \frac{1-B^2}{1+B^2} \sqrt{A^2 - B^2}$	③
ETCH-RATE RATIO $V \equiv \frac{V_T}{V_B}$	7'	$V(R) = \frac{\Delta L(R)}{\Delta h}$	① ②
	8'	$V = \frac{\left[(1-B^2)^2 + 4A^2\right]^{1/2}}{1 - B^2}$; $B \equiv \frac{d}{2h}$; $A \equiv \frac{D}{2h}$;	②
	9'	$V(x_o) = \frac{1}{\sin\delta(x_o)} = \left[1 + \frac{1}{[f'(x)]^2}\right]^{1/2}$	④
	10'	$V(x_o) = \frac{1}{\cos 2\beta}$; $x_o = h - \frac{d(h)}{2\tan 2\beta}$	⑤
	11'	$V = \frac{1}{\sin\delta}$ where $\cos\delta\left(\sqrt{n^2 - \cos^2\delta} - \sin\delta\right) = \sin\Phi$, n = refractive index	⑥

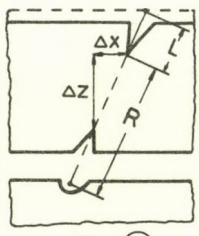

Fig.①

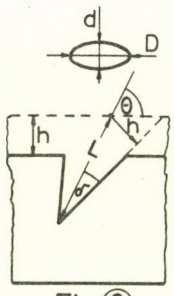

Fig.②

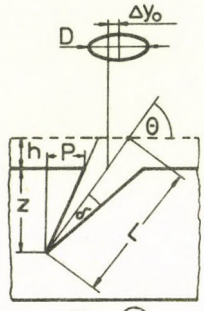

Fig.③

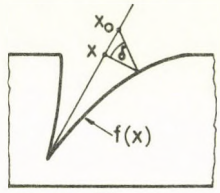

Fig.④

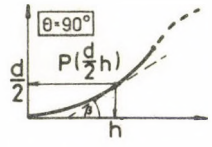

Fig.⑤

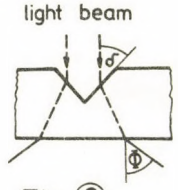

Fig.⑥

Table IV. Formulas for calculating the layer removal, h_p, at the moment of perforation of a thin isotropic foil in case of constant etch-rate ratio.

cases for V=const	S_1	S_2	T_1	T_2	T_3
h_p =	$\frac{l_o}{V \sin\theta}$	$l_o = R_o\left(\sin\theta - \frac{1}{V}\right)$	$\frac{1}{2} \cdot \frac{l_o}{V\sin\theta}$	$\frac{l_o}{2} - \frac{R_o}{2}\left(\sin\theta - \frac{1}{V}\right)$	
valid if	$l_o \leq R_o\sin\theta$	$0 \leq R_o\sin\theta \leq l_o$	$l_o \leq R_o\sin\theta$	$0 \leq R_o\sin\theta \leq l_o - \frac{R_o}{V}$	$l_o - \frac{R_o}{V} \leq R_o\sin\theta \leq l_o$

$V \equiv v_T/v_B$, R_o = range, l_o = original thickness of foil, $\sin\theta > \frac{1}{V}$.

Table V. Formulas for calculating the layer removal, h_p, at the moment of perforation of a thin isotropic foil in case of varying etch-rate ratio

cases for V≠ const	S_1	S_2	T_1 and T_1'	T_2	T_3
h_p=	$\int_{x_c}^{l_o/\sin\theta} V^{-1}dx + h_c$	$l_o - R_o\sin\theta + \int_{x_c}^{R_o} V^{-1}dx + h_c$	$\frac{1}{2}\int_{x_c}^{l_o/\sin\theta} V^{-1}dx + \frac{h_c}{2}$	$\frac{l_o}{2} - \frac{1}{2}\left(R_o\sin\theta - \int_{x_c}^{R_o} V^{-1}dx\right) + \frac{h_c}{2}$	
valid if	$l_o \leq R_o\sin\theta$	$0 \leq R_o\sin\theta \leq l_o$	$l_o \leq R_o\sin\theta$	$0 \leq R_o\sin\theta \leq l_o - h_c - \int_{x_c}^{R_o} V^{-1}.dx$	$l_o - h_c - \int_{x_c}^{R_o} V^{-1}dx \leq R_o\sin\theta \leq l_o$

$x_c = h_c/\sin\theta$, h_c = critical layer removal, $\sin\theta > \frac{1}{V_{max}}$

Table VI. Formulas for describing etch-hole minor axes[×] in thin isotropic foils at constant etch-rate ratio

ETCH SITUATION	FORMULAS	VALID[+] IF	ETCH-HOLE CONTOUR[×]
S_1	$d_1(S_1) = 2\,\frac{h V\sin\theta - l_o}{\sqrt{(V\sin\theta)^2 - 1}}$	$h_p(S_1) \leq h \leq l_o$	 growing ellipse
S_2	$d_1(S_2) = 2\sqrt{\left(h - \frac{R_o}{V}\right)^2 - (l_o - R_o\sin\theta)^2}$	$h_p(S_2) \leq h \leq h_t(S_2) \equiv \frac{R_o}{V} + (l_o - R_o\sin\theta)\,V\sin\theta$	 growing circle, then circle portion linked with growing ellipse portion
	$d_2(S_2) = d_1(S_1)$	$h_t(S_2) \leq h \leq l_o$	 semicircle and semi-ellipse, then ellipse portion linked with diminishing circle portion[++]
T_1	$d_1(T_1) = \frac{2hV\sin\theta - l_o}{\sin\theta\sqrt{V^2 - 1}}$	$h_p(T_1) \leq h \leq h_t(T_1) \equiv \frac{l_o}{2}\,\frac{2 - \frac{B}{\sin\theta}}{V\sin\theta + 1 - VB}$	 growing circle, then if $d > (l_o - 2h)/\cos\theta$, a complex spatial configuration with the indicated projected shape
	$d_2(T_1) = 2\,\frac{hV\sin\theta + h - l_o}{\sqrt{(V\sin\theta)^2 - 1}}$	$h_t(T_1) \leq h \leq \frac{l_o}{2}$	
T_2	$d_1(T_2) = 2\sqrt{\left(h - \frac{R_o}{V}\right)^2 - (l_o - h - R_o\sin\theta)^2}$	$h_p(T_2) \leq h \leq h_t(T_2) \equiv \frac{h_t(S_2)}{V\sin\theta + 1}$	 growing circle, then circle portion linked with growing ellipse portion
	$d_2(T_2) = d_2(T_1)$	$h_t(T_2) \leq h \leq \frac{l_o}{2}$	 semicircle and -ellipse, then ellipse portion with diminishing circle portion
T_3	$d_1(T_3) = \frac{(2h - l_o)V + R_o(V\sin\theta - 1)}{\sqrt{V^2 - 1}}$	$h_p(T_3) \leq h \leq h_t(T_3) \equiv \frac{l_o}{2}\,.\,\frac{2 - VB + \frac{R_o}{l_o}(V\sin\theta - 1)B}{V\sin\theta + 1 - VB}$	 see the remark for $d_1(T_2)$
	$d_2(T_3) = d_2(T_1)$	$h_t(T_3) \leq h \leq \frac{l_o}{2}$	 see the remark for $d_2(T_2)$

+ h_p = layer removal at the moment of foil perforation (see in Table IV.)
h_t = layer removal at the moment of transition, i.e. when the hole contour is just composed of a semiellipse and semicircle.

$$B = \sqrt{\frac{(V\sin\theta)^2 - 1}{V^2 - 1}}$$

++ The total ellipse contour can not develop if $l < V\cos\theta$

× The contour and minor axis are considered in the plane of back surface of the foil for S_1, S_2 and T_2, and for T_1 and T_3 in the plane of interception of the two connecting track cones

Table VII. Formulas for describing etch-hole diameters at the back /support/ and top surfaces of a stripping film for varying etch-rate ratio in case of normal incidence of particle to the detector surface.

	ETCH SITUATION	FORMULAS	VALID IF
BACK SURFACE	$l_o \leq R_o$	$d(s_1) = 2(l_o - x_o)\sqrt{V^2(x_o) - 1}$ $h = H(x_o) + (l_o - x_o)V(x_o)$	$H(l_o) \leq h \leq l_o$ $H(l_o) \equiv \int_0^{l_o} V^{-1}(x)\,dx$
	$0 \leq R_o \leq l_o$	$d_1(s_2) = 2\sqrt{(h - H(R_o))^2 - (l_o - R_o)^2}$	$H(R_o) + l_o - R_o \leq h \leq h_t(s_2)$
		$d_2(s_2) = 2(l_o - x_o)\sqrt{V^2(x_o) - 1}$ $h = H(x_o) + (l_o - x_o)V(x_o)$	$h_t(s_2) \leq h \leq l_o$ $h_t(s_2) \equiv H(R_o) + V(R_o)(l_o - R_o)$
TOP SURFACE	$l_o \leq R_o$	$d(t_1) = 2(x_o - H(x_o))\sqrt{\frac{V(x_o)+1}{V(x_o)-1}}$ $h = x_o + \frac{x_o - H(x_o)}{V(x_o) - 1}$	$0 \leq h \leq l_o$
	$0 \leq R_o \leq l_o$	$d_1(t_2) = 2(x_o - H(x_o))\sqrt{\frac{V(x_o)+1}{V(x_o)-1}}$ $h = x_o + \frac{x_o - H(x_o)}{V(x_o) - 1}$	$0 \leq h \leq h_t(t_2)$ $h_t(t_2) \equiv R_o + \frac{R_o - H(R_o)}{V(R_o) - 1}$
		$d_2(t_2) = 2\sqrt{(h - H(R_o))^2 - (h - R_o)^2}$	$h_t(t_2) \leq h \leq l_o$

The Editorial Board acknowledges that this supplement has been edited by the author.

Kiadja a
Magyar Tudományos Akadémia
Atommag Kutató Intézete

A kiadásért és szerkesztésért felelős
Dr. Somogyi György

Készült az ATOMKI nyomdájában
Törzsszám:11431
Debrecen,1979/2
Példányszám:580

ПРИЛОЖЕНИЕ

АТОМКІ

СООБЩЕНИЯ

ТОМ 21 № 2

SUPPLEMENT

ATOMKI BULLETIN

Volume 21 Number 2